High-Accuracy Indoor Ranging Using Microwave OFDM Signals

Mehmet Yazgan, *Graduate Student Member, IEEE*, Hüseyin Arslan, *Fellow, IEEE*, and Stavros Vakalis, *Member, IEEE*

***Abstract*— High-accuracy wireless ranging and positioning becomes necessary in many applications, and while many waveforms promise high accuracy, their performance in cluttered environments is not optimal. This article confers about the potential of high-accuracy wireless ranging using orthogonal frequency-division multiplexing (OFDM) signals. The excellent correlation properties of OFDM signals for high-accuracy ranging in real-life environments are discussed and the Cramer–Rao lower bound (CRLB) is derived for OFDM ranging independent of the transmitted information. Simulation results and experimental measurements at a carrier frequency of 1.4 GHz with 200 MHz of bandwidth are included. Range estimation is demonstrated with a standard deviation of 1.6 mm in a realistic laboratory environment with no anechoic walls.**

***Index Terms*— Correlation, Cramer–Rao lower bound (CRLB), high-accuracy ranging, joint radar–communication, orthogonal frequency-division multiplexing (OFDM), radar.**

I. Introduction

WIRELESS ranging and positioning is crucial for various applications, including wireless sensor networks [1], navigation [2], robotics [3], and indoor localization where global navigation satellite system (GNSS) lacks precision, necessitating short-range localization systems [4].

Joint radar and communications (JRC) has gained attention due to enabling greater spectrum efficiency and cost-effectiveness [5]. This integration is significant for structural monitoring, smart building management, indoor positioning, and security systems within indoor environments, providing real-time data transmission and target detection for assessing the integrity and safety of buildings [6], [7], [8]. Achieving JRC involves coexistence, which increases cost and interference [9], or codesign that includes either communication or radar-centric waveforms [10]. Using traditional radar waveforms, such as frequency-modulated continuous wave (FMCW), causes significant challenges. Those are designed primarily for radar sensing, and their characteristics may not be optimal for data transmission [11]. In addition, multiplexing between FMCW and other communications waveforms limits the data rate achieved for communication purposes [12]. Hence, this study concentrates on the sensing performance of orthogonal frequency-division multiplexing (OFDM), a fundamental and promising technique in current and upcoming wireless communication systems [13], [14]. Thus, this work is concerned with high-accuracy ranging using OFDM signals, using the waveform directly for sensing without any modification [15], [16]. Therefore, the proposed approach will not impact communication performance and demonstrates excellent ranging accuracy. Despite many studies showcasing the efficacy of OFDM signals in radar applications [17], their potential for high-accuracy ranging and positioning remains relatively unexplored and necessitates experimental validation in a realistic environment [18]. We examine the OFDM signal correlation properties and present the theory of wireless OFDM ranging, including a straightforward derivation of the Cramer–Rao lower bound (CRLB) largely independent of the transmitted information [19]. Real-life experimental measurements using OFDM signals that achieve a 1.6-mm standard deviation are included along with simulations.

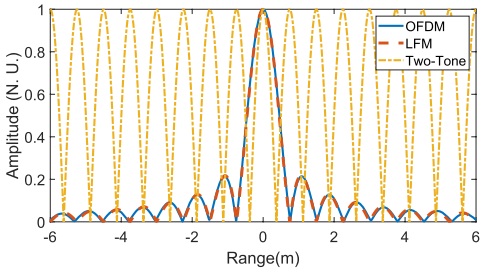

Fig. 1. Comparison of autocorrelation responses: two-tone waveform (200-MHz separation), LFM, and OFDM (200-MHz bandwidth).

II. Wireless Ranging Using OFDM Signals

Recent high-accuracy-ranging radar advancements have leveraged two-tone waveforms and wideband linear frequency-modulated (LFM) signals. While two-tone waveforms offer optimal accuracy, their autocorrelation (yellow) is highly ambiguous for multiple targets as shown in Fig. 1. OFDM signals (blue) exhibit excellent correlation properties similar to LFM (orange), making them valuable for range estimation, localization, and dual radar–communications waveform in fifth-generation (5G) networks [20], [21], [22], [23].

Received 6 June 2024; revised 5 August 2024; accepted 20 September 2024. Date of publication 7 October 2024; date of current version 6 December 2024. *(Corresponding author: Stavros Vakalis.)*

Mehmet Yazgan and Stavros Vakalis are with the Department of Electrical Engineering, University of South Florida, Tampa, FL 33620 USA (e-mail: myazgan@usf.edu; vakalis@usf.edu).

Hüseyin Arslan is with the Department of Electrical and Electronics Engineering, Istanbul Medipol University, Istanbul 34810, Türkiye (e-mail: huseyinarslan@medipol.edu.tr).

Color versions of one or more figures in this letter are available at https://doi.org/10.1109/LMWT.2024.3468230.

Digital Object Identifier 10.1109/LMWT.2024.3468230

The baseband time-domain OFDM signal with N subcarriers can be written as $s(t) = \sum_{n=1}^{N} A_n e^{j\phi_n} e^{j2\pi n \Delta f t}$, where A_n and ϕ_n represent the symbol amplitude and phase on the nth subcarrier, respectively, and Δf denotes the subcarrier spacing. Subsequently, it is quadrature upconverted to a carrier frequency f_c, and then transmitted. Assuming a target at distance R, the scattered signal $r(t)$ after quadrature downconversion is represented by $r(t) = \sum_{n=1}^{N} \alpha_n A_n e^{j\phi_n} e^{j2\pi(n\Delta f)(t-\tau)} + w(t)$, where α_n is the complex channel response at the nth subcarrier, $w(t)$ denotes the receiver noise, $\tau = (2R/c)$ corresponds to round-trip time delay, and c is the speed of light. We use a matched filter for range estimation, maximizing the signal-to-noise ratio (SNR) at its output instead of subcarrier processing. Unlike other works [24], matched filtering includes one OFDM symbol with N subcarriers at a time to avoid sidelobes. The matched filter output can be given by $x(\tau) = \int_{-T}^{T} s^*(t-\tau) r(t) dt$. Matched filtering, or pulse compression, provides processing gain and enhances output SNR without the distortion of multiple amplification chains [25]. Considering signal bandwidth B and duration T, the time–bandwidth product, $k = B \cdot T$, is the matched filter processing gain [26] and depends on the number of subcarriers. The time delay estimate $\hat{\tau}$ maximizes the matched filter response magnitude, yielding a range estimate $\hat{R} = c\hat{\tau}/2$. The range resolution R_{res} is inversely proportional to B and equal to $c/(2 \cdot B) = c/(2 \cdot N\Delta f)$. With OFDM symbol duration $T_s = 1/\Delta f$, excluding cyclic prefix (CP), the maximum unambiguous range is inversely proportional to subcarrier spacing [27]

$$R_{\text{un}} = \frac{c \cdot T_s}{2} = \frac{c}{2 \cdot \Delta f}. \tag{1}$$

The CP at the beginning of an OFDM signal, a duplicated signal part, can create ambiguity. CP removal is common practice in OFDM receiver processing which does not eliminate the CP from reflections off secondary targets situated at greater distances, as expressed in Section IV. The standard deviation of range estimates, a crucial metric for this work, is discussed next.

III. OFDM CRLB Derivation

The CRLB gives a lower bound for the variance of an unbiased estimator [28], [29]. This work looks for a formulation independent of the OFDM symbol information. For the problem of time delay estimation, the CRLB becomes

$$\sigma_{\hat{\tau}}^2 \geq \frac{N_0/2}{\beta^2 E_s} \tag{2}$$

where N_0 is the noise power spectral density, E_s is the signal energy, and β^2 is the mean-squared bandwidth, which can be written as $\beta^2 = (\int_{-\infty}^{\infty} (2\pi f)^2 |R(f)|^2 df)/(\int_{-\infty}^{\infty} |R(f)|^2 df)$. For an OFDM signal that uniformly occupies the bandwidth B, the following approximation can be made $|R(f)| \approx |R_\mu| \text{rect}(f/B)$, where $R(f)$ is the received signal spectrum and $|R_\mu| = (1/B) \int_{-(B/2)}^{(B/2)} |R(f)| df$ is the mean absolute value. This approximation is particularly valid for lower order modulation types but can become less accurate for higher modulation orders such as 256 quadrature amplitude modulation (256-QAM) where the OFDM spectrum has larger amplitude variations. The two integrals can be calculated as $\int_{-\infty}^{\infty} (2\pi f)^2 |R(f)|^2 df \approx \int_{-(B/2)}^{(B/2)} (2\pi f)^2 |R(f)|^2 df \approx |R_\mu|^2 (\pi^2 B^3)/3$, and $\int_{-\infty}^{\infty} |R(f)|^2 df \approx \int_{-(B/2)}^{(B/2)} |R(f)|^2 df \approx |R_\mu|^2 B$ [29]. Therefore

$$\sigma_{\hat{\tau}}^2 \geq \frac{3N_0/2}{\pi^2 B^2 E_s} \tag{3}$$

and since $(E_s/N_0) = \text{SNR} \cdot T_{\text{ofdm}} \cdot f_s$, SNR is the per-symbol SNR, the sampling frequency f_s is equal to B, and T_{ofdm} is the duration of one OFDM symbol including CP, which results in

$$\sigma_{\hat{\tau}}^2 \geq \frac{3}{2\pi^2 B^3 T_{\text{ofdm}} \text{SNR}}. \tag{4}$$

T_{ofdm} is equal with $(1 + K_{\text{cp}})(1/\Delta f) = N(1 + K_{\text{cp}})(1/B)$, where K_{cp} is the CP rate. Hence, $N(1 + K_{\text{cp}})$ represents the length of the whole OFDM symbol. Converting time delay into round-trip range estimates $\hat{R}$ using the range estimation formula defined in Section II, we find

$$\sigma_{\hat{R}}^2 \geq \frac{3c^2}{8\pi^2 \cdot B^2 \cdot N\left(1 + K_{\text{cp}}\right) \cdot \text{SNR}}. \tag{5}$$

Increasing signal bandwidth and SNR reduces the variance in range estimates. In addition, increasing K_{cp} and the number of subcarriers extends the symbol duration, decreasing variance. Increased bandwidth also reduces packet synchronization errors, which, although minor in communication, can negatively impact range estimation. Reducing the sampling period by increasing bandwidth can mitigate this issue. However, due to spectral limitations, a user might not always be able to increase the bandwidth. In such cases, oversampling on the receiver side can reduce the impact of synchronization errors.

IV. Simulations and Experimental Measurements

The experimental measurements were conducted indoors at the University of South Florida using OFDM signals generated by a Keysight M8190 AWG at 1.4 GHz with a 200-MHz bandwidth, 4-QAM digital modulation, and 3.125-MHz subcarrier spacing. All these parameters were also exploited in simulations. Signals were captured using a Keysight MXR404A Oscilloscope, with the transmitter and receiver using COMPOWER AH-118 Double Ridge Horn Antennas.

Monte Carlo simulations (3000 iterations) in MATLAB were performed for single- and multiple-target scenarios. First, a single target at 3.273 m was simulated to match the experimental conditions. Then, multi-target ranging was simulated with targets at 3.273, 6, and 9 m. Fig. 2(a) depicts the matched filter output. Sidelobes in matched filtering can negatively affect the accuracy of neighboring range estimates, leading to a higher standard deviation than in the single target case. The matched filter response is separately highlighted in Fig. 2(b) to exhibit the sidelobe impact readably. Even the smallest ripples due to clutter can increase the variance, emphasizing the importance of selecting a waveform with excellent correlation properties. In the experiment, range estimation using a digital matched filter identified the target at

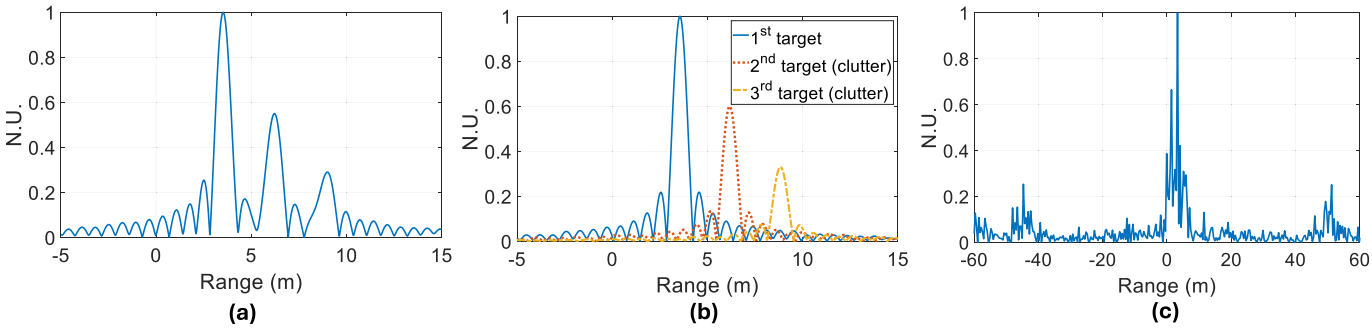

Fig. 2. (a) Simulated matched filter output of multi-target ranging. (b) Single-target simulated matched filter output of the target (blue) and clutter (orange and yellow). (c) Matched filter output of experimental OFDM measurements with a target located at 3.273 m.

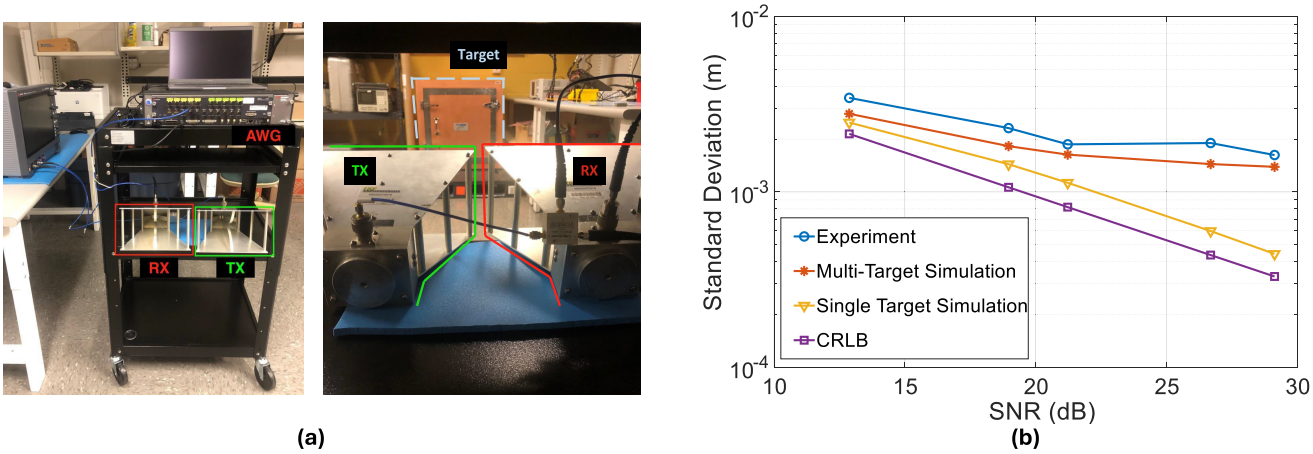

Fig. 3. (a) (Left) Photograph of the experimental setup: Tx antenna in green, red shows Rx antenna. (Right) Object in gray at a distance of 3.273 m. (b) Standard deviation of the simulated and experimental measurements as a function of SNR. The experimental system achieves a standard deviation of 1.6 mm at SNR = 29.13 dB.

3.273 m, as shown in Fig. 2(c). Antenna coupling occurred at 1.39 m, with potential ambiguities at −44.69 and 51.24 m due to the CP. Since the CP is a small portion of the received OFDM symbol, the amplitude levels of ambiguities are low. According to (1), the theoretical unambiguous range of 48 m aligns with the observed R_{un} in Fig. 2(c), based on subcarrier spacing. While the CP is removed after packet synchronization in OFDM systems, its effects can still pose challenges in multi-target ranging. In non-restricted environments, where targets can be at arbitrary ranges, the CP can introduce significant ambiguity. This is because the CP of the first echo is removed but a portion of the signals' CP reflected from other targets will remain since the maximum excess delay can longer be than CP duration. Therefore, investigating and mitigating the effects of CP is critical for accurate ranging in such scenarios. In practical indoor environments, this ambiguity is minor unless the maximum excess delay is longer than CP duration.

The setup is shown in Fig. 3(a), with the left image depicting the experimental setup and the right image displaying the antennas observing the target, an ETS Lindgren Shielded Test Box, located 3.273 m away. The simulated and experimental standard deviations versus SNR are given in Fig. 3(b), alongside a CRLB comparison. CRLB is plotted as the square root of (5) for K_{cp} and N equal to 1/4, and 64, respectively. The standard deviation of single-target simulation (yellow) closely aligns with the CRLB (purple) in the absence of multipath, as illustrated in Fig. 3(b). In multi-target cases, echoes from additional targets (clutter) induce higher variance (orange) due to the sidelobe impact as mentioned earlier in this section. The standard deviation of the experimental measurements is shown in blue. SNR was varied by adjusting the transmit power of the AWG. SNR estimation in the experiment was done using the known power spectral density and measurement of the noise floor. The OFDM bandwidth is $N \cdot \Delta f$, and OFDM symbol length $T_{\text{ofdm}} = (1 + K_{\text{cp}})(1/\Delta f)$. Hence, the matched filtering processing gain is 80 corresponding to $N(1 + K_{\text{cp}})$ which results in no required amplifier in the experiment. At an SNR of 29.13 dB, with Tx and Rx power values of 2.64 dBm and −30.58 dBm, respectively, we achieve a standard deviation of 1.6 mm. Although some studies show a lower ranging standard deviation, they do not use communication waveforms, and their measurements are conducted in anechoic environments.

V. Conclusion

This research demonstrates the effectiveness of OFDM waveforms for highly accurate indoor ranging in real-life cluttered environments, emphasizing the potential for integrated communications and sensing. Despite the high peak-to-average power ratio (PAPR) issue in OFDM systems [30], various methods such as clipping, selective mapping, and block coding mitigate this problem [31]. Hence, this article focuses on experimentally validating OFDM systems for high-accuracy ranging, with future work exploring JRC tradeoffs.

REFERENCES

[1] N. Patwari, J. N. Ash, S. Kyperountas, A. O. Hero, R. L. Moses, and N. S. Correal, "Locating the nodes: Cooperative localization in wireless sensor networks," *IEEE Signal Process. Mag.*, vol. 22, no. 4, pp. 54–69, Jul. 2005.

[2] Y. Zhuang and N. El-Sheimy, "Tightly-coupled integration of WiFi and MEMS sensors on handheld devices for indoor pedestrian navigation," *IEEE Sensors J.*, vol. 16, no. 1, pp. 224–234, Jan. 2016.

[3] K.-C. Chen, S.-C. Lin, J.-H. Hsiao, C.-H. Liu, A. F. Molisch, and G. P. Fettweis, "Wireless networked multirobot systems in smart factories," *Proc. IEEE*, vol. 109, no. 4, pp. 468–494, Apr. 2021.

[4] A. Cidronali, G. Collodi, S. Maddio, M. Passafiume, and G. Pelosi, "2-D DoA anchor suitable for indoor positioning systems based on space and frequency diversity for legacy WLAN," *IEEE Microw. Wireless Compon. Lett.*, vol. 28, no. 7, pp. 627–629, Jul. 2018.

[5] C. Baquero Barneto et al., "Full-duplex OFDM radar with LTE and 5G NR waveforms: Challenges, solutions, and measurements," *IEEE Trans. Microw. Theory Techn.*, vol. 67, no. 10, pp. 4042–4054, Oct. 2019.

[6] X. Wan et al., "Joint radar and communication empowered by digital programmable metasurface," *Adv. Intell. Syst.*, vol. 4, no. 9, Sep. 2022, Art. no. 2200083.

[7] Y. Cao and Q. Yu, "A joint beamforming design and integrated CPM-LFM signal for dual-functional radar-communication systems," 2021, *arXiv:2112.09825*.

[8] Y. Quan, L. Shi, J. Liu, and J. Ma, "A novel bistatic joint radar-communication system in multi-path environments," in *Proc. 12th Int. Conf. Commun. Softw. Netw. (ICCSN)*, Jun. 2020, pp. 186–191.

[9] J. A. Zhang et al., "Enabling joint communication and radar sensing in mobile networks—A survey," *IEEE Commun. Surveys Tuts.*, vol. 24, no. 1, pp. 306–345, 1st Quart., 2022.

[10] S. Rafique and H. Arslan, "A novel frame design for integrated communication and sensing based on position modulation," in *Proc. IEEE 94th Veh. Technol. Conf.*, Sep. 2021, pp. 1–5.

[11] B. Paul, A. R. Chiriyath, and D. W. Bliss, "Survey of RF communications and sensing convergence research," *IEEE Access*, vol. 5, pp. 252–270, 2016.

[12] M. Nemati, Y. H. Kim, and J. Choi, "Toward joint radar, communication, computation, localization, and sensing in IoT," *IEEE Access*, vol. 10, pp. 11772–11788, 2022.

[13] L. Zhao et al., "Transmission of 1024-QAM OFDM at 28 GHz radio frequency using 5G millimeter wave phased array antenna," *IEEE Trans. Microw. Theory Techn.*, vol. 70, no. 9, pp. 4211–4217, Sep. 2022.

[14] J. Yli-Kaakinen et al., "Frequency-domain signal processing for spectrally-enhanced CP-OFDM waveforms in 5G new radio," *IEEE Trans. Wireless Commun.*, vol. 20, no. 10, pp. 6867–6883, Oct. 2021.

[15] S. Vakalis, L. Gong, and J. A. Nanzer, "Imaging with WiFi," *IEEE Access*, vol. 7, pp. 28616–28624, 2019.

[16] S. Vakalis, S. Mghabghab, and J. A. Nanzer, "Fourier domain millimeter-wave imaging using noncooperative 5G communications signals," *IEEE Trans. Antennas Propag.*, vol. 70, no. 10, pp. 8872–8882, Oct. 2022.

[17] J. Wang, P. Wang, R. Zhang, and W. Wu, "SDFnT-based parameter estimation for OFDM radar systems with intercarrier interference," *Sensors*, vol. 23, no. 1, p. 147, Dec. 2022, doi: 10.3390/S23010147.

[18] R. Qian, D. Jiang, and W. Fu, "Digital constant-envelope modulation scheme for radar using multicarrier OFDM signals," *IET Signal Process.*, vol. 11, no. 7, pp. 861–868, Sep. 2017.

[19] T. Wang, Y. Shen, S. Mazuelas, H. Shin, and M. Z. Win, "On OFDM ranging accuracy in multipath channels," *IEEE Syst. J.*, vol. 8, no. 1, pp. 104–114, Mar. 2014.

[20] A. Schlegel, S. M. Ellison, and J. A. Nanzer, "A microwave sensor with submillimeter range accuracy using spectrally sparse signals," *IEEE Microw. Wireless Compon. Lett.*, vol. 30, no. 1, pp. 120–123, Jan. 2020.

[21] O. Abari, H. Rahul, D. Katabi, and M. Pant, "AirShare: Distributed coherent transmission made seamless," in *Proc. IEEE Conf. Comput. Commun. (INFOCOM)*, Aug. 2015, pp. 1742–1750.

[22] C. Gu and J. Lien, "A two-tone radar sensor for concurrent detection of absolute distance and relative movement for gesture sensing," *IEEE Sensors Lett.*, vol. 1, no. 3, pp. 1–4, Jun. 2017.

[23] H. Mahmoud, T. Yucek, and H. Arslan, "OFDM for cognitive radio: Merits and challenges," *IEEE Wireless Commun.*, vol. 16, no. 2, pp. 6–15, Apr. 2009.

[24] C. Sturm and W. Wiesbeck, "Waveform design and signal processing aspects for fusion of wireless communications and radar sensing," *Proc. IEEE*, vol. 99, no. 7, pp. 1236–1259, Jul. 2011.

[25] M. Oelze, "Bandwidth and resolution enhancement through pulse compression," *IEEE Trans. Ultrason., Ferroelectr., Freq. Control*, vol. 54, no. 4, pp. 768–781, Apr. 2007, doi: 10.1109/TUFFC.2007.310.

[26] B. R. Mahafza, *Radar Systems Analysis and Design Using MATLAB*. Boca Raton, FL, USA: CRC Press, 2005.

[27] C. Sturm, E. Pancera, T. Zwick, and W. Wiesbeck, "A novel approach to OFDM radar processing," in *Proc. IEEE Radar Conf.*, May 2009, pp. 1–4.

[28] S. M. Kay, *Fundamentals of Statistical Signal Processing: Estimation Theory*. Upper Saddle River, NJ, USA: Prentice-Hall, 1993.

[29] S. Prager, M. S. Haynes, and M. Moghaddam, "Wireless subnanosecond RF synchronization for distributed ultrawideband software-defined radar networks," *IEEE Trans. Microw. Theory Techn.*, vol. 68, no. 11, pp. 4787–4804, Nov. 2020.

[30] M. Yasmeen, "A modified approach based on SLM for OFDM PAPR reduction using time domain SubBlock conversion matrix," *Int. J. Recent Innov. Trends Comput. Commun.*, vol. 3, no. 4, pp. 1900–1904, 2015.

[31] Y. A. Jawhar et al., "A review of partial transmit sequence for PAPR reduction in the OFDM systems," *IEEE Access*, vol. 7, pp. 18021–18041, 2019.